# Chapter 6. Microtremor studies

## 6.1 Introduction

Geological, structural and microstructural investigations within the Champaner Group suggest that the waning phase of deformation and latest metamorphic event are related with emplacement of Godhra granite. In order to study the said relationship, the subsurface mapping of the pluton morphology becomes most essential.

Several geophysical methods viz. gravity (Bott 1955; Vigneresse 1990; Singh et al. 2004; Rao et al. 2006; Cruden 2008; Singh et al. 2014), magnetic (Mamtani and Greiling 2005); aeromagnetic (Sahu 2012) magnetotelluric (Sastry et al. 2008); deep resistivity soundings (Singh et al. 2008); and deep seismic methods (Kaila et al. 1981; Dixit et al. 2010) have been used for sub-surface investigations.

Microtremor studies is the cost-effective seismic method, which can map subsurface rheological boundaries due to its strong acoustic impedance along contrasting density at sediment/ rock interphases at shallower depths and across fault zones (Kanai 1957; Yamanaka et al. 1994; Ibs-Vonseht and Wohlenberg 1999; Delgado et al. 2000a, b; Parolai et al. 2002; Garcia-Jerez et al. 2006; Guéguen et al. 2006; Zhao et al. 2007; Dinesh et al. 2010; Rošer and Gosar 2010; Sukumaran et al. 2011; Paudyal et al. 2013). Microtremor technique runs on the ambient noise that contain the fundamental resonant frequency of near surface sediment horizons (Ohta et al. 1978; Celebi et al. 1987; Lermo et al. 1988; Nakamura 1989; Field et al. 1990; Hough et al. 1991; Yamanaka et al. 1994; Konno and Ohmachi 1998; Ibs-Vonseht and Wohlenberg 1999; Delgado et al. 2000a, b; Aki and Richards 2002). The derived resonating frequencies correspond with the velocity of the seismic wave and the sediment thickness (Ibs-Vonseht and Wohlenberg 1999; Parolai et al. 2002).

---

* This chapter is based on our paper published:
(a) Joshi, A U, Sant, D A, Parvez, I A, Rangarajan, G, Limaye, M A, Mukherjee, S, Charola, M J, Bhatt, M N, Mistry, S P (2018) Subsurface profiling of granite pluton using microtremor method: southern Aravalli, Gujarat, India. International Journal of Earth Sciences, vol. 107, pp. 191-201. (doi: 10. 1007/s00531-017-1482-9).

The ratio of the horizontal (NS + EW) and vertical (H/V) component of the noise spectrum is used to normalize the source effect and to amplify the seismic wave (Nogoshi and Igarashi, 1971).

In present chapter, author discusses the application of Microtremor method to establish relationship between granite pluton with Champaner meta-sediments in terms their deformation. Studying neighboring Lunavada region, Mamtani et al., (2005) concluded that the emplacement of Godhra granites are synchronous, which results into the pluton deformation, or at times post dates the regional deformation resulting into doming up of sequences (Denele et al., 2014). The resulting domes are majority governed by the pluton shapes. These shapes are at times circular or wedge-shaped, flat-floored or disk shaped, sometimes sheeted or even resembles a hockey puck. For elaborative descriptions of other forms see (McSween and Harvey 1997; Benn et al. 1998; Vigneresse et al. 1999).

Bundelkhand tectonic zone (Rahman and Zainuddin, 1993; Chauhan et al., 2018), Capricon Orogen of western Australia (Tyler and Thorne, 1990); The late Svecofennian granite-migmatite zone of southern Finland (Ehlers et al., 1993); Pan-African belt of central Africa (Njiekak et al., 2008) and Granite-greenstones belts of North China Craton (Tang and Santosh, 2018) are the few sites that exemplifies granite emplacements and deformation.

The Champaner terrain provides an opportunity to study the relationship of pluton emplacement and its deformation with the country rocks, due to the presence of domes within it. One such dome near Narukot and its western extension provides an array, which cuts the axial plane of all major fold trends. In case of the Champaner terrain a cost-effective microtremor method was employed to portray the sub-surface morphology of the granite pluton underneath the Narukot dome and to its western extension. Moreover, the technique was useful in determining the overall vertical thickness of the meta-sedimentary litho-units belonging to the Champaner Group.

## 6.2 Methodology

A Lennartz seismometer of 5 second period and a City Shark-II data acquisition system have been deployed to acquire the ambient noise. The collected ambient noise has three components, viz. N-

S, E-W and vertical directions. The recording was carried out for 40 min at the rate of 100samples/second/ site (Sukumaran et al. 2011). All the 32 geophysical stations (Fig. 6.1) arrayed for measurement run almost parallel to the axial trace (N95°) of the Narukot Dome. The station interval was decided considering topography along the profile line. The region with rolling topography from station 1–13 was surveyed at 1 km interval, whereas the rugged terrain, stations 13–32 (Fig. 6.1), was surveyed at 500 m interval. The large portion of the profile encounters meta-sedimentaries and granite along with minor occurrences of Mesozoic sedimentaries and Daccan basalts.

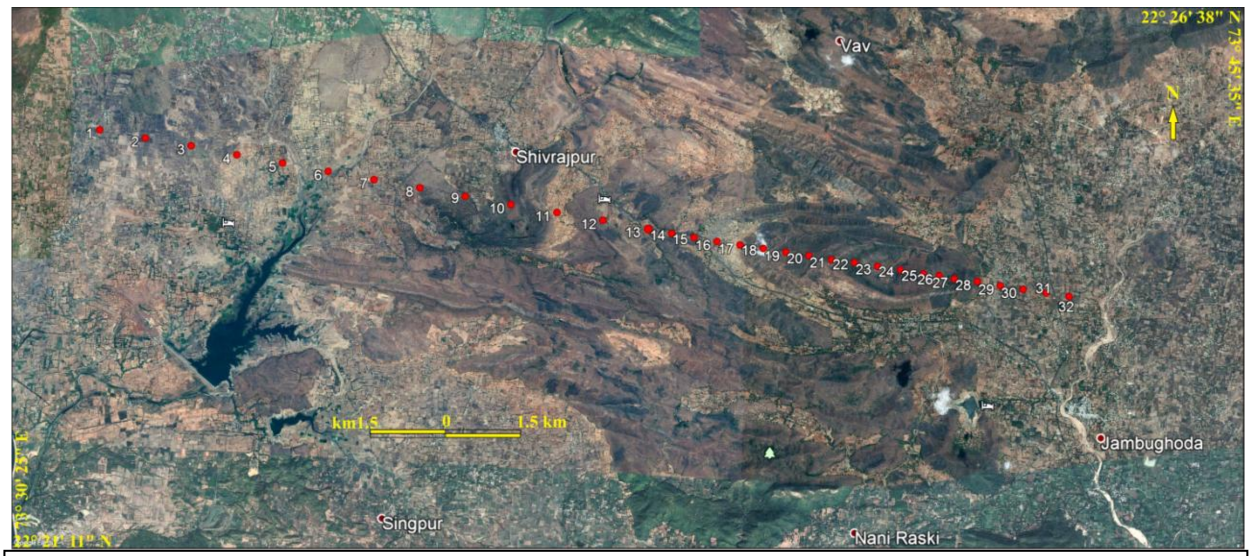


Figure 6.1: Geo-eye image of the Champaner terrain; source: google-earth software. Oval structure along the E margin represents the Narukot Dome. Dotted line across the dome and further W shows locations of 1-32 stations for microtremor measurements.

### 6.3 Results

The ratio between the Fourier amplitude spectra of the horizontal to the vertical (H/V) components of persisting Rayleigh waves were calculated from the ambient noise vibrations acquired from 32 stations using the GEOPSY software (SESAME European Project 2004). The H/V spectralratios were plotted between 0.2 and 25 Hz encompassing the complete range of resonating frequencies recorded within the study area. These H/V ratios were further processed individually to identify statistically significant spectral peaks using custom-written Matlab code. The statistically significant peaks were taken to be those peaks that were at least one standard deviation greater than the baseline activity. These peaks then correspond to significant fundamental resonating frequencies for each station. The significant fundamental resonating frequencies $f_0$, $f_1$ and $f_2$ were singled out for individual stations quantifying their amplitudes (Fig. 6.2; Table. 6.1). Figure. 6.2 illustrates a series of H/V spectral frequency plots recorded from the study area. Station 5, 6, 12, 13, 17, 22, 23, 24, 26, 30 and 31 show the peaks at fundamental frequency ($f_0$). Station 1, 2, 3, 4, 7, 8, 9 and 10 show dual frequency ($f_{0,}$ $andf_1$) with representing the boundary at both deeper and shallower levels; station 11, 14, 15, 19, 20, 25, 27, 28 and 29 also show dual frequency ($f_{0,}$ $andf_1$) but at different frequencies that correspond to the interphases at moderate to shallower depth level. However, station 16, 18, 21, and 32 represent three frequencies ($f_0$,$f_1$, $f_2$) incorporating 3 interphases at shallow, moderate and deeper levels.

The thickness (*h*) of soil/sediment layer over the bed rock can be related theoretically with the fundamental resonant frequency ($f_r$) of H/V spectral ratio (Ibs-Vonseht and Wohlenberg 1999)

$$h = af_r^{\,b}, \qquad (1)$$

where, a and b are obtained by nonlinear regression betweenthe thickness and the fundamental resonant frequency.

(1)$f_0$= 0.2328; $f_1$=0.9130

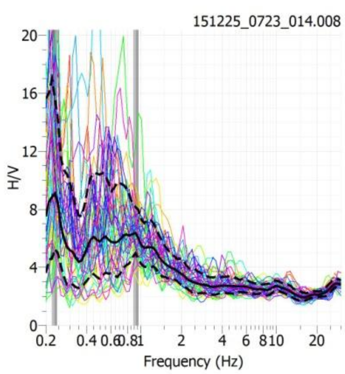


(2)$f_0$=0.9130; $f_1$=18.0848

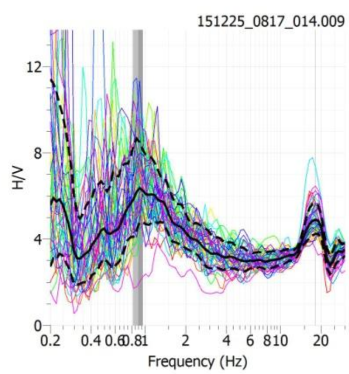


(3)$f_0$=0.7088; $f_1$=18.0848

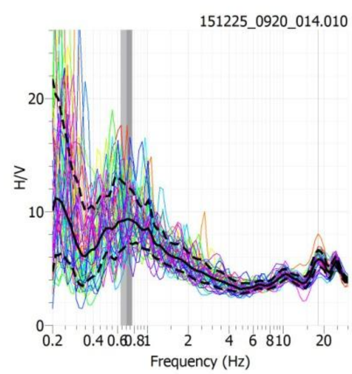

(4)$f_0$=1.1759; $f_1$=0.2328

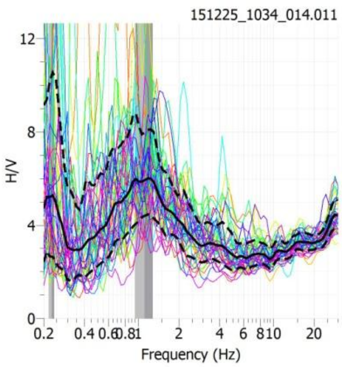


(5)$f_0$=0.2328

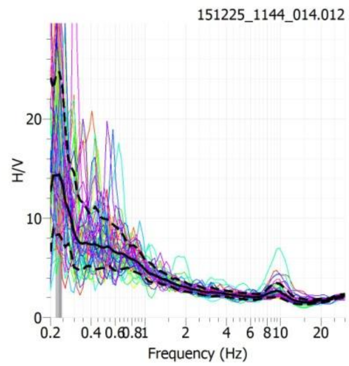


(6)$f_0$=0.221937

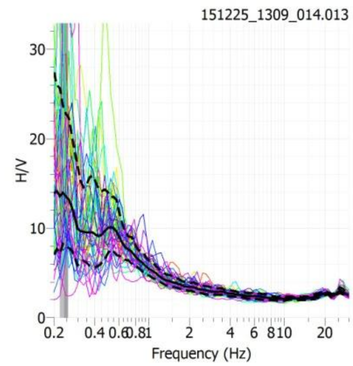


(7)$f_0$=12.6896; $f_1$=1.3011

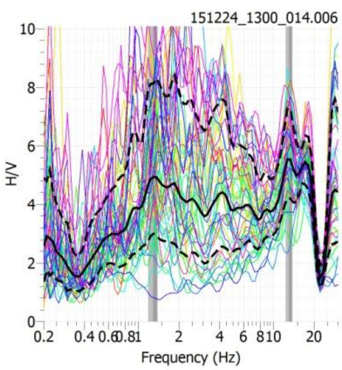


(8)$f_0$=1.3011; $f_1$=25.7738

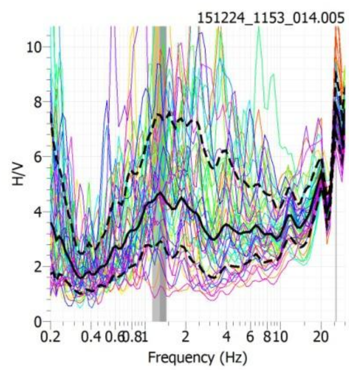


(9)$f_0$=1.18284; $f_1$=12.3244

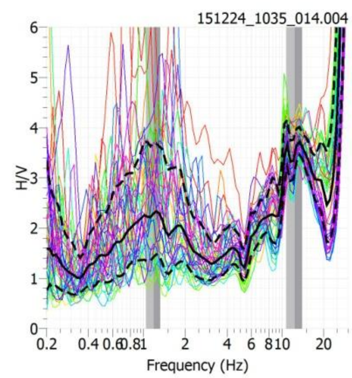


(10)$f_0$=0.7456; $f_1$=25.7738

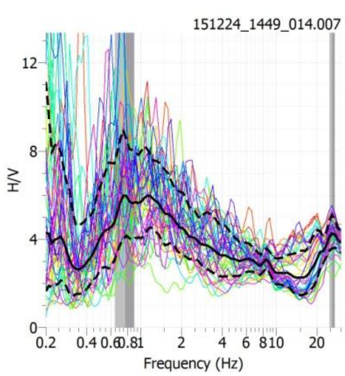


(11)$f_0$=27.1119; $f_1$=1.1759

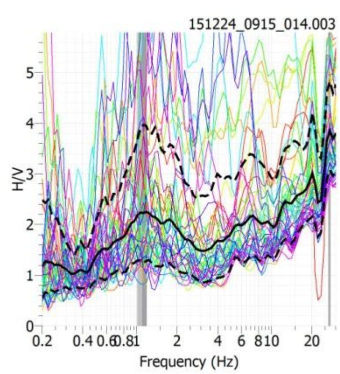


(12)$f_0$=12.6896

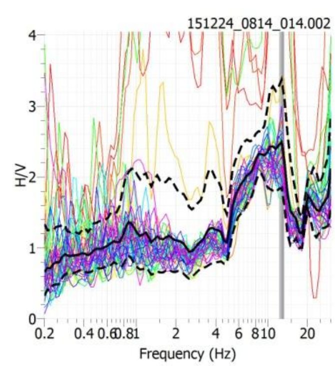

(13)$f_0$=18.0848

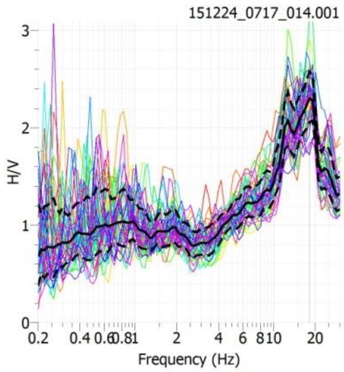


(14)$f_0$=10.9020; $f_1$=1.31352

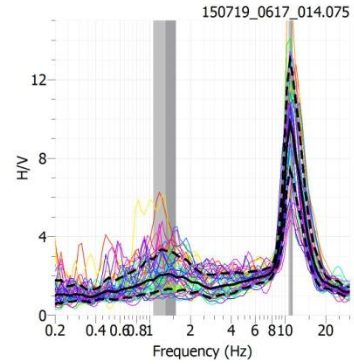


(15)$f_0$=9.3662; $f_1$=1.3687

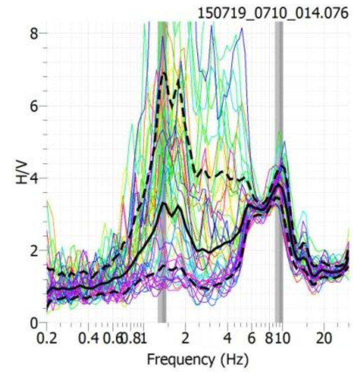


(16)$f_0$=8.9040; $f_1$=18.0848; $f_2$=1.2369

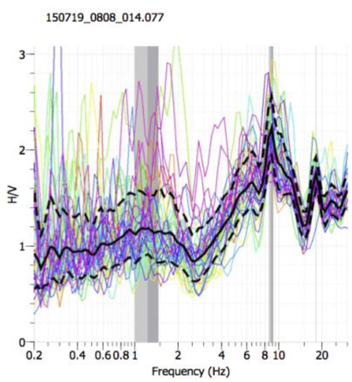


(17)$f_0$=14.7704

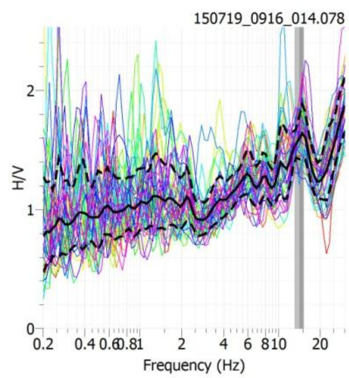


(18)$f_0$=1.8543; $f_1$=25.7738; $f_2$=4.3838

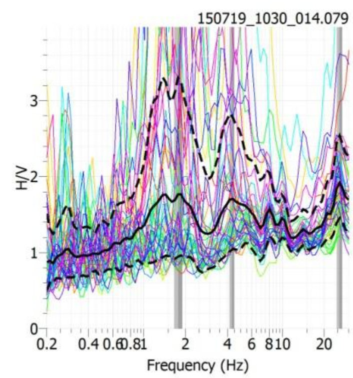


(19)$f_0$=1.5145; $f_1$=20.0113

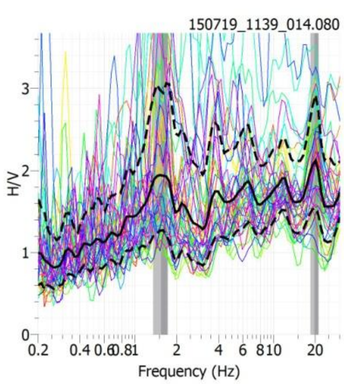


(20)$f_0$=10.3640; $f_1$=1.6758

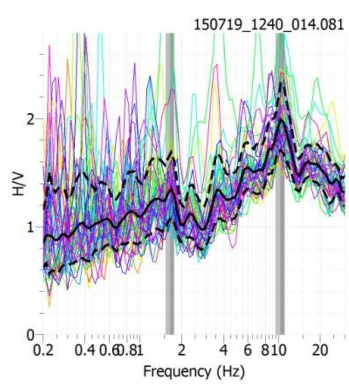


(21)$f_0$=27.1119; $f_1$=19.0237; $f_2$=1.9035

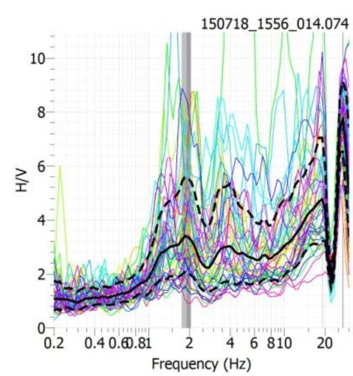

(22)$f_0$=6.5720

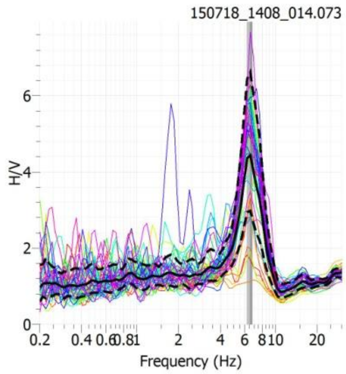


(23)$f_0$=1.8543

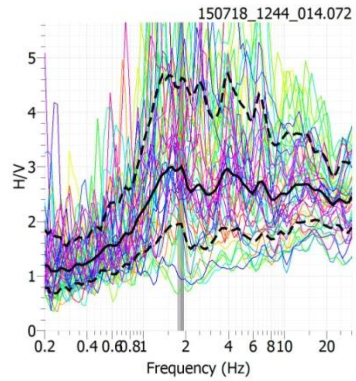


(24)$f_0$=1.4397

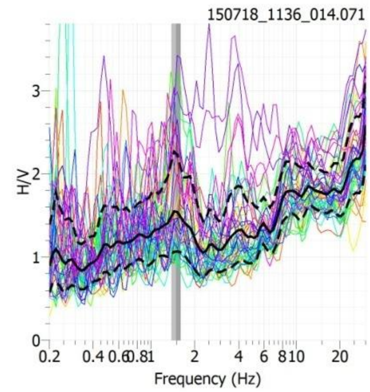


(25)$f_0$=18.0848; $f_1$=1.46282

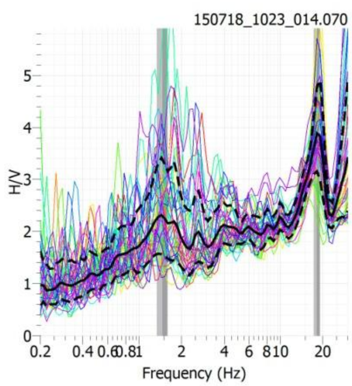


(26)$f_0$=18.0848

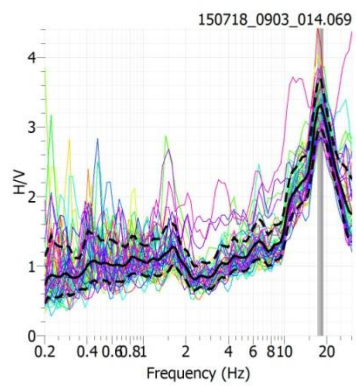


(27)$f_0$=19.0237; $f_1$=8.33

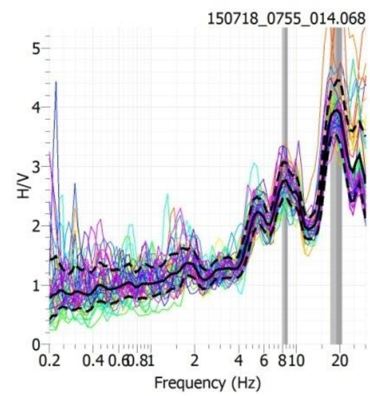


(28)$f_0$=5.3676; $f_1$=1.8

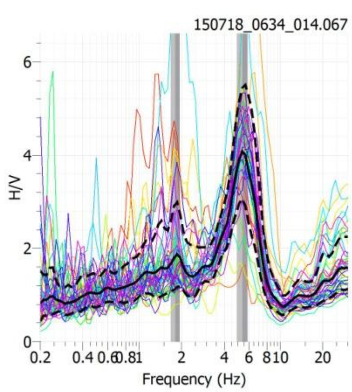


(29)$f_0$=8.4645; $f_1$=1.4397

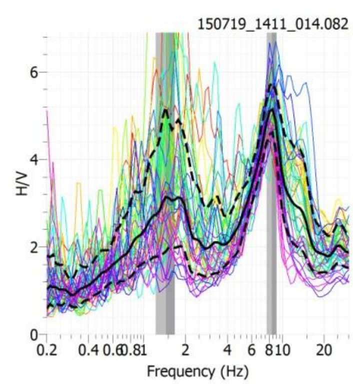


(30)$f_0$=10.9020

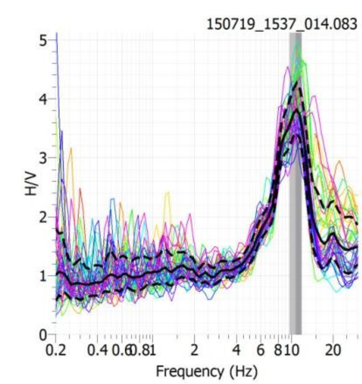

(31)$f_0$=10.3640

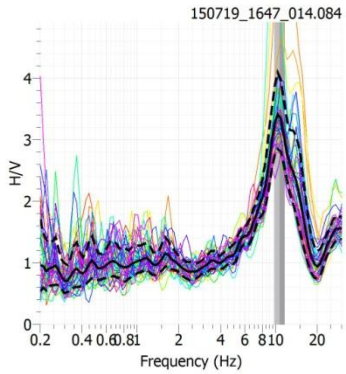


(32)$f_0$=1.3687; $f_1$=6.9132; $f_2$=25.7738

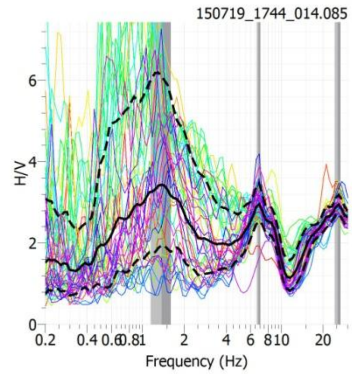


Figure 6.2: H/V spectral frequency plot recorded for 1-32 stations from the study area ((1), (2)... indicate station numbers). Station 5, 6, 12, 13, 17, 22, 23, 24, 26, 30 and 31 show the peaks at fundamental frequency ($f_0$); station 1, 2, 3, 4, 7, 8, 9 and 10 show dual frequency ($f_{0,}$ and$f_1$) with representing the interphases at both deeper and shallower levels; station 11, 14, 15, 19, 20, 25, 27, 28 and 29 also show dual frequency ($f_{0,}$ and $f_1$) but at different frequencies that correspond to the interphases at moderate to shallower depth level. However, station 16, 18, 21, and 32 represent three frequencies ($f_0$, $f_1$, $f_2$) incorporating 3 interphases at shallow, moderate and deeper levels.

Table 6.1: Fundamental resonant frequency $f_0$, $f_1$ *and* $f_2$ for station 1 to 32 across Narukot Dome and in its western extension along a WNW profile. The depths of rheological boundaries are calculated using Eq. 3 ($h = 56.8 f_r^{-1}$: derived from borehole data from station 29 whereas Eq. 4 ($h = 58.3 \pm 8.8 f_r^{-0.95 \pm 0.1}$: Dinesh et al., 2010).

| *Stations* | $f_o$ | *Depth in m ( Eq 3)* | *Depth in m (Eq 4)* | $f_1$ | *Depth in m ( Eq 3)* | *Depth in m (Eq 4)* | $f_2$ | *Depth in m ( Eq 3)* | *Depth in m (Eq 4)* |
|---|---|---|---|---|---|---|---|---|---|
| 1 | 0.2328 | 243.814 | 232.828 | 0.913 | 62.169 | 63.565 | | | |
| 2 | 0.913 | 62.169 | 63.565 | 18.0848 | 3.139 | 3.726 | | | |
| 3 | 0.7088 | 80.079 | 80.848 | 18.0848 | 3.139 | 3.726 | | | |
| 4 | 1.1759 | 48.269 | 49.982 | 0.2328 | 243.814 | 232.828 | | | |
| 5 | 0.2328 | 243.814 | 232.828 | | | | | | |
| 7 | 12.6896 | 4.473 | 5.217 | 1.3011 | 43.625 | 45.402 | | | |
| 8 | 1.3011 | 43.625 | 45.402 | 25.7738 | 2.202 | 2.661 | | | |
| 9 | 1.18284 | 47.986 | 49.704 | 12.3244 | 4.605 | 5.363 | | | |
| 10 | 0.7456 | 76.127 | 77.053 | 25.7738 | 2.202 | 2.661 | | | |
| 11 | 27.1119 | 2.094 | 2.536 | 1.1759 | 48.269 | 49.982 | | | |
| 12 | 12.6896 | 4.473 | 5.217 | | | | | | |
| 13 | 18.0848 | 3.139 | 3.726 | | | | | | |
| 14 | 10.902 | 5.206 | 6.026 | | | | | | |
| 15 | 9.3662 | 6.060 | 6.961 | 1.3687 | 41.470 | 43.269 | | | |
| 16 | 8.904 | 6.375 | 7.304 | 18.0848 | 3.139 | 3.726 | 1.2369 | 45.889 | 47.638 |
| 17 | 14.7704 | 3.843 | 4.516 | | | | | | |
| 18 | 1.8543 | 30.610 | 32.426 | 25.7738 | 2.202 | 2.661 | 4.3838 | 12.948 | 14.319 |
| 19 | 1.5145 | 37.478 | 39.302 | 20.0113 | 2.836 | 3.384 | | | |
| 20 | 10.364 | 5.477 | 6.323 | 1.6758 | 33.870 | 35.699 | | | |
| 21 | 27.1119 | 2.094 | 2.536 | 19.0237 | 2.984 | 3.551 | | | |
| 22 | 6.572 | 8.637 | 9.747 | | | | | | |
| 23 | 1.8543 | 30.610 | 32.426 | | | | | | |
| 24 | 1.4397 | 39.425 | 41.239 | | | | | | |
| 25 | 18.0848 | 3.139 | 3.726 | | | | | | |
| 26 | 18.0848 | 3.139 | 3.726 | | | | | | |
| 27 | 19.0237 | 2.984 | 3.551 | | | | | | |
| 28 | 5.3676 | 10.575 | 11.813 | | | | | | |
| 29 | 8.4645 | 6.706 | 7.664 | 1.4397 | 39.425 | 41.239 | | | |
| 30 | 10.902 | 5.206 | 6.026 | | | | | | |
| 31 | 10.364 | 5.477 | 6.323 | | | | | | |
| 32 | 1.3687 | 41.470 | 43.269 | 6.9132 | 8.210 | 9.289 | 25.7738 | 2.202 | 2.661 |

For a given fundamental resonant frequency, if the velocity of seismic waves ($V_s$) for a given interphase is known, the depth of the interphases is given by Parolai et al.(2002):

$$h = V_s / 4f_r \, , \tag{2}$$

On the other hand, if the depth of the interphase in known based on available core record, the velocity of seismic waves ($V_s$) can be determined using Eq. (2).

In the present study, a record of 300 ft (91.4 m) private borehole data was used, existing nearer to station 29, in Hirapur Village, east of Narukot dome. The records suggest 7 ft (2.13 m) thick soil unit, followed by 15 ft (4.57 m) thick white fine-grained sand (alteration product of in situ granite); and 278 ft (84.7 m) of massive granite. The categorization of both the soil unit and altered granite unit were done as regolith. Using the observed depth of regolith–granite boundary (6.70 m), $V_s$ as 227 m/s for the regolith unit at station 29 was computed using Eq. (2). The depth of regolith–granite boundary for stations 28, 30, 31 and 32 has been estimated using the above computed value of $V_s$. In addition, substituting the value of $V_s$ in Eq. 2, equation 3 has been derived from the study area.

$$h = (56.8) f_r^{-1} \tag{3}$$

Equation (3) is comparable to the equation derived for a granitic terrain around Bangalore (state Karnataka, India) decoding interphase of soil–regolith from that of granites (Dinesh et al. 2010), viz.

$$h = (58.3 \pm 8.8) f_r^{-0.95 \pm 0.1} \tag{4}$$

In the present context, author preferred to use the equation established by Dinesh et al. (2010) to derive theoretical depths of interphases as they had established the relationship using a larger number of observed borehole logs.

Further, grouping fundamental resonating frequency, geology and structural data from the study area, two distinct rheological boundaries were identified, viz. (i) 0.2219–10.364 Hz that is inferred to record boundary between Champaner metasediment and granites (C–Gr boundary) and (ii) 10.902–27.1119 Hz that differentiates phyllites from quartzites (P–Qr boundary) (Figs. 6.3, 6.4). The other boundaries identified along the western margin of the profile, viz. (iii) 0.7088-12.6896 Hz frequencies distinguish the boundary between the Champaner metasediments and the Mesozoic sediments. On the other hand, at stations 2 and 3, (iv) 18.0848 Hz frequency distinguishes thin Deccan traps from Mesozoic sediments.

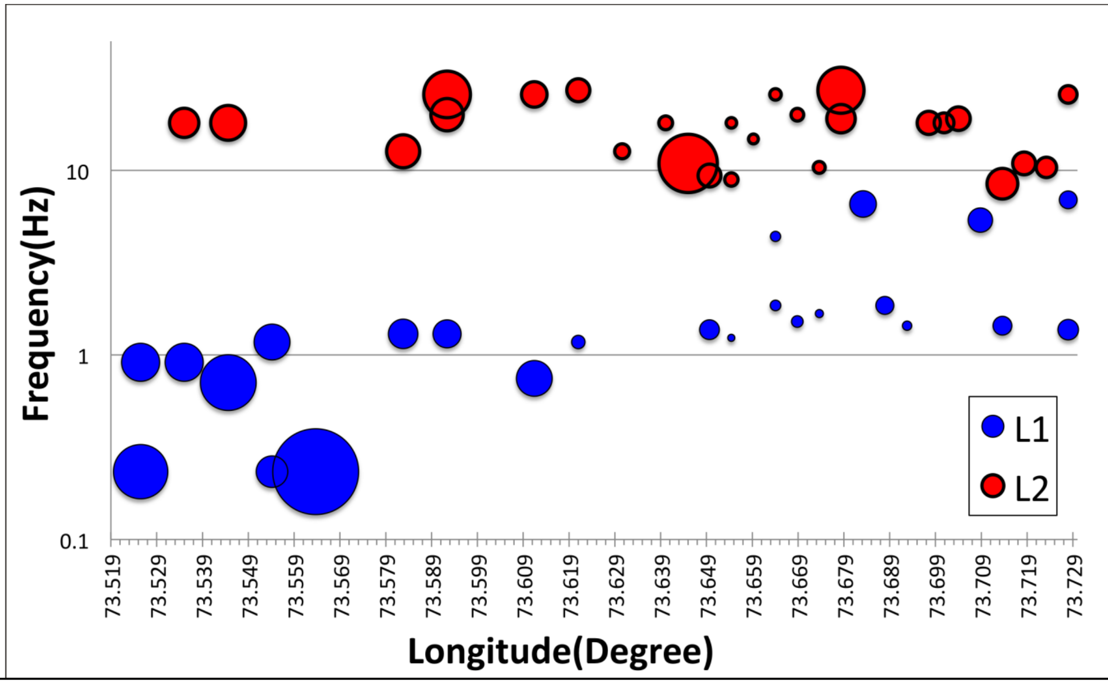


Figure 6.3: Fundamental resonant frequency of 1 to 32 stations along WNW trending profile. The diameter of bubbles captures amplitude of fundamental resonant frequency. The blue colour represent frequency for C-Gr boundary (L1) that ranges between 0.2219-10.364 Hz, whereas red colour represents frequency for P-Qr boundary (L2) that ranges between 10.902-27.1119 Hz.

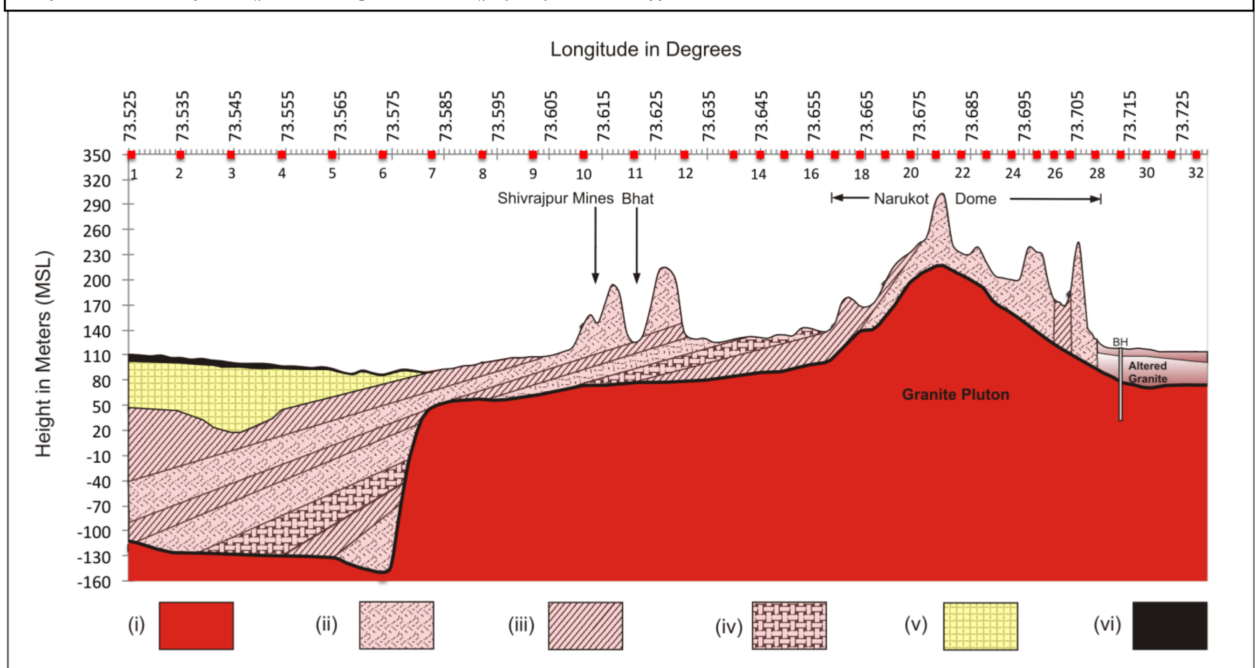


Figure 6.4: Layered model for the profile along Narukot Dome and to its W. Subsurface interphases of C-Gr and P-Qr plotted with reference to the surface elevation. C-Gr boundary shows the granite pluton hump (from station 16 to 29) towards eastern part of the profile. The C-Gr interphase in W distinguishes a steep wall of the pluton (between stations 6 and 7) taking pluton further deeper to 243.64 m (station 6) and 232.82 m (station 1). The P-Qr boundary shows a steep plunge E of the granite pluton hump and 15° gentle plunge due W. The profile highlights sub-surface extension of the Champaner Group further W overlain by Mesozoic sedimentaries and thin cover of Deccan basalt between stations 1 and 7. Numbers in the figure indicate *(i)* Granites, *(ii)* Quartzites, *(iii)* Phyllites, *(iv)* Conglomerates, *(v)* Mesozoic sedimentaries, *(vi)* Deccan basalt.

***(i) Champaner–granite boundary***

The Champaner–granite boundary (C–Gr boundary) occurs at a shallower depth towards E than at the W margin of the profile showing an arched-up geometry (Fig. 6.4). The granite pluton attains shallowest depth calculated from surface underneath station 20 (35.69 m) and station 23 (32.42 m) followed by a significant depth, or a ‘low’, beneath station6 (243.64 m) and station 1 (232.82 m) towards W. C–Gr boundary follows a steep slope between stations 7 (45.40 m)and 6 (243.64 m). The low along profile between stations 1and 6 marks an extension of the younger Champaner rocks exposed around stations 7 and 8 (Rajgarh Formation) and is confirmed based on aeromagnetic data (Sahu 2012).

***(ii) Phyllite–quartzite boundary***

The phyllite–quartzite (P–Qr boundary) sequence of Champaner Group is well exposed in the western extension of Narukot dome. During the field studies, boundary of different lithology and their trends were recorded and mapped. Lithology and structural trends were plotted along the topographic profile, extrapolating their contact up to the C–Gr boundary (Fig. 6.4).

***(iii & iv) Other rheological boundaries***

In the western portion of the profile, the C–Gr boundary is ~240 m deep. The Rajgarh Formation in this part directly overlies granites deduced from aeromagnetic data (Sahu 2012). The boundary between the Rajgarh Formation and Mesozoic sediments is ~70 m deep. The boundary between the Mesozoic sediments and Deccan basalt is ~1–2 m deep (Fig. 6.4).

## 6.4 Inferences

The microtremor study reveals Champaner–granite boundary as the most conspicuous rheological boundary that emphasizes the morphology of subsurface granite pluton (Fig. 6.4).The granitic pluton forms a hump between stations 29 and 16 followed by gentle westerly dip up to station 7. The profile between stations 6 and 7 highlights a steep wall of the granite pluton, with 230-m deep C–Gr boundary, thereafter follows a rolling topography till station 1. On the other hand, the Champaner metasediment terminates abruptly above granite plutons imparting a discordant relation. The sporadic granitic plutons emplaced in the terrain presumably uprooted the Champaner metasediments giving "rootless" characteristic especially at Narukot dome and to its western extension. Further east of the Narukot dome, at Jothwad (Gol Dungri) such rootless character can be deciphered (Joshi and Limaye, 2018). To present the relation between the pluton and associated deformation, a geological cross-section across Narukot Dome and its extension towards W has been prepared, by extrapolating surface geology and structural trends up to regolith–granite rheological boundaries delineated by microtremor studies (Fig. 6.4). The sporadic emplacement of plutonic bodies produced asymmetric plunge along the dome. The Champaner metasediments between stations 23 and 29, E of the pluton hump, display steep WSW plunge, whereas the pluton hump at station 20, metasediments show gentle plunge of 15° towards west.

The estimated vertical thickness of Champaner metasediments varies as: 30 m (station 20), 100 m (station 21) and goes to a maximum of136 m (station 12) at the Shivrajpur Manganese Mine. In the W extension of Narukot dome, the estimated thickness of Rajgarh Formation is ~108 m followed by 70-m thick Mesozoic sediment capped by 1–1.5-m thick Deccan basalt.

--------END--------